Beam Squint in Ultra-wideband mmWave Systems: RF Lens Array vs. Phase-Shifter-Based Array

Sang-Hyun Park, *Student Member, IEEE*, Byoungnam Kim, *Member, IEEE*, Linglong Dai, *Senior Member, IEEE*, Dong Ku Kim, *Senior Member, IEEE*, Kai-Kit Wong, *Fellow, IEEE*, and Chan-Byoung Chae, *Fellow, IEEE*

***Abstract*—In this paper, we investigate the beam-squint in the radio frequency (RF) lens of ultra-wideband millimeter-wave (mmWave) systems. We compare, in terms of the beam-squint, the proposed RF lens antenna with the phase shifter-based array in hybrid-beamforming scheme. To reduce the hardware and channel matrix complexities for full digital beamforming, researchers have introduced an RF lens-based hybrid beamforming scheme. The use of mmWave systems, however, causes an increase in bandwidth, which gives rise to beam-squint. Beam-squint can, in the analog beamforming area, misalign beams. We find the causative factors for beam-squint in the RF lens antenna. Based on the beamforming gain at each frequency, we verify that the RF lens is free of the beam-squint effect in a specific situation by analyzing causative factors and assessing throughput. For the analysis, we first numerically interpret the beam-squint of each antenna type using 3D electromagnetic analysis software. Based on the results, we present the degraded spectral efficiency by system-level simulations with 3D indoor ray tracing. Finally, to verify our analysis, we fabricate an actual RF lens antenna and demonstrate the real performance using an mmWave, NI PXIe, software-defined radio system.**

***Index Terms*—Beam-squint, mmWave, lens antenna, hybrid beamforming, analog beamforming, software-defined radio, 3D ray tracing.**

I. Introduction

In future fifth-generation (5G) cellular networks, the required data rate is expected to be 1000 times greater than that of fourth-generation (4G) cellular networks. To overcome the diminishing amount of frequency bandwidth and to meet the increasing data-rate demands, both academia and industry need to undergo a paradigm shift from the sub-6 GHz systems to millimeter wavelength (mmWave, 30–300 GHz) [1]. In its technical reports [2], the 3rd Generation Partnership Project (3GPP) has already announced the 3 GHz bandwidth (26.5–29.5 GHz). An ultra-wideband range, the 3 GHz bandwidth has not been used in the sub-6 GHz frequency spectrum. Using mmWave in cellular networks is different from using sub-6 GHz bands owing to unique characteristics of mmWave. In particular, the mmWave is vulnerable to obstacles and large-distance path losses. This vulnerability has led researchers to investigate, over the past few decades, multiple-input multiple-output (MIMO) systems so as to provide higher capacity gains and better link reliabilities [3]. In mmWave systems having shorter wavelengths than the sub-6 GHz range, more antenna elements can be integrated for the same array size. Thus, to overcome the path loss of mmWave, engineers can use more antenna elements per unit size than that of sub-6 GHz. In full digital beamforming (BF), though, as the number of antenna elements increases in the front end, the complexity of channel matrix computation increases exponentially. Furthermore, as antenna elements require dedicated radio frequency (RF) chains [4], the hardware complexity increases as well. The application of phase-shifting to multiple data streams after the baseband to form a highly directed beam is called analog-digital hybrid BF. The hybrid BF achieves array and multiplexing gains simultaneously [5]. In general, the array gain is proportional to the array size and number of antenna elements. Therefore, the array gain has advantages in mmWave massive MIMO systems. Between performance and hardware cost, though, the hybrid BF is subject to a trade-off, according to a new approach proposed in [6], [7]. According to the authors in [6] and [7], the RF lens antennas can reduce the hardware complexity without incurring performance degradation. In the proposed hybrid BF, the RF lens is placed at the front end of the antenna array (see Fig. 1). The results in the studies verify that the lens antenna, while reducing hardware complexity, achieves the conventional high gain and directivity with lens-focusing characteristics.

A major problem still to solve for hybrid BF, though, is beam-squint. Beam-squint refers to the phenomenon in which the beam-steering angle is altered depending on the operating frequency [8]. The phase of each antenna element must be shifted to steer the analog BF in a specific direction. Because the wave number influences the array factor of the phased array, the operating frequency band alters the analog BF angle. Fig. 1 presents the RF lens and phase shifter-based ultra-wideband hybrid BF structure and the beam-squint phenomenon. Mis-aligned beams (colored in red and blue) caused by beam-squint do not cover the user equipment (UE). Since these beams are incredibly narrow in a large array hybrid-BF system, the beam-squint phenomenon can be a critical issue that affects the received power. The RF lens and the phased array both generate beam-squint, though their causes differ. In the former, the cause is the frequency-dependent permittivity of the RF lens and in the latter the same steering vector of the phased array. We detail this in Section II-A. In the same vein, beam-squint has been studied as a factor that degrades performance in hybrid BF systems [9]. The authors in [9] present beam-squint suppression methods, but these solutions

S.-H. Park, D. K. Kim, C.-B. Chae are with Yonsei University, Seoul, Korea (e-mail: {williampark,dkkim, cbchae}@yonsei.ac.kr).

B. Kim is with Sensor View, Gyeonggi-do, Korea (e-mail: klaus.kim@sensor-view.com).

L. Dai is with Tsinghua University, Beijing, China (e-mail: daill@tsinghua.edu.cn).

K.-K. Wong is with University College London, UK. (e-mail: kai-kit.wong@ucl.ac.uk).

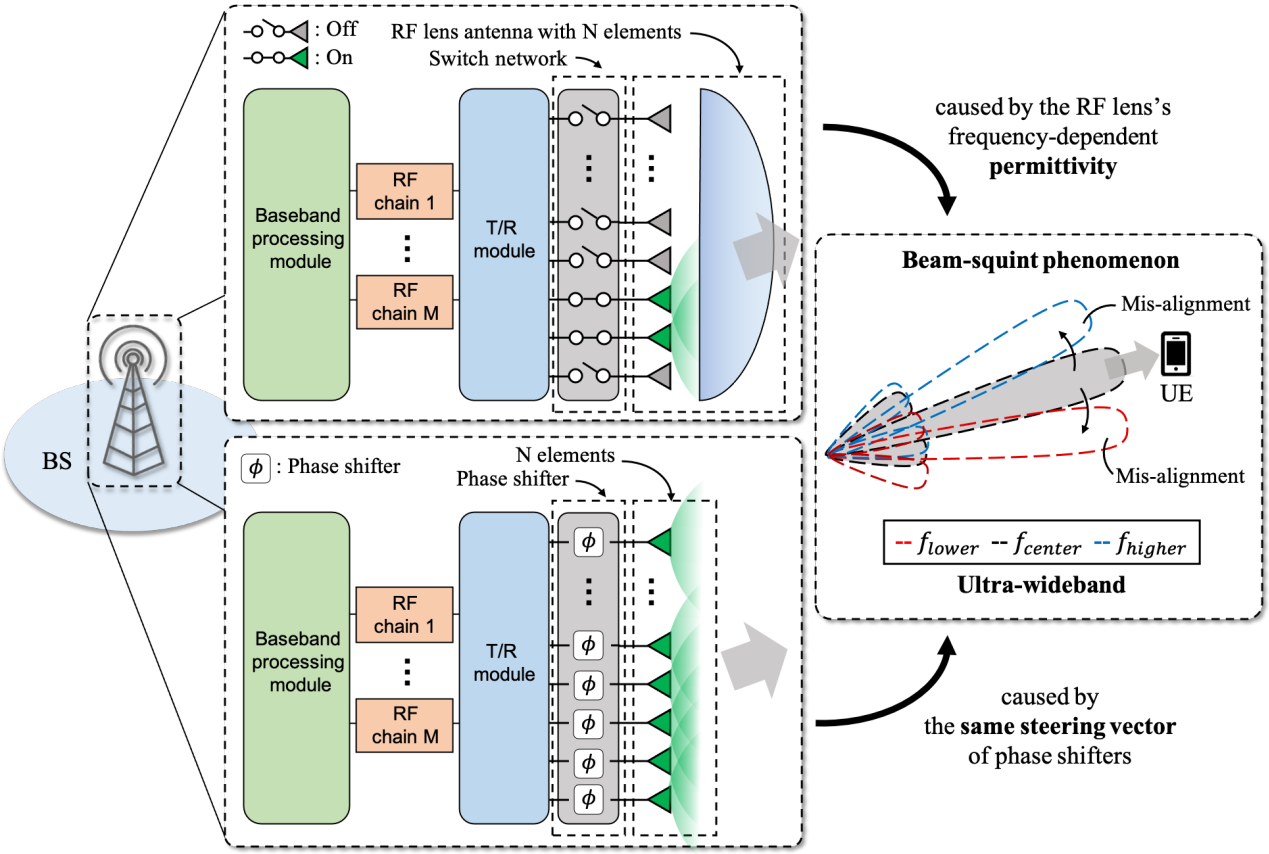

Figure 1. The hybrid BF system structures and the beam-squint phenomenon of the RF lens and the phase shifter-based array. f_{lower}, f_{center}, and f_{higher} denote lower frequency, center frequency, and higher frequency, respectively.

still have a trade-off between performance and hardware cost.

Consequently, a combination of mmWave ultra-wideband systems and hybrid BF produces beam-squint, which causes a limitation in cellular networks. The authors in [10] considered beamspace channel estimation for the mmWave wideband. By exploiting the effect of beam-squint caused by the wideband, the authors proved that each path component of the wideband beamspace channel shows a unique frequency-dependent sparse structure. However, for the RF lens antenna applied to wireless communications over a short period, researchers have yet to publish work on either the causative factors of beam-squint in the RF lens antenna or the resulting throughput degradation. Therefore, we present here the causes of the beam-squint phenomenon and its performance assessment for the convex RF lens antenna.

The remainder of this paper is organized as follows. Section II presents the inherent causative factor of beam-squint in the RF lens and the phased array. Section III presents the system model used in the 3D EM analysis software. In addition, we introduce the BF gain ratio that assesses the beam-squint effects; we also classify and summarize causative factors that cause the beam-squint phenomenon. In Section IV, we first present the results of an indoor, map-based 3D ray-tracing method for accurate analysis of the beam-squint. We verify the degraded spectral efficiency and received power ratio of the fabricated RF lens through the NI mmWave software-defined radio (SDR) platform over the air. Finally, we summarize our results, contributions, and propose future works.

II. Beam-squint in the RF lens antenna

A. Why Does Beam-squint Occur in Lens Antenna Structure?

In this section, we explain the reason why the beam-squint phenomenon occurs in RF lens antennas. Beam-squint is generated by the complex, material permittivity of the RF lens, which is a function of operating frequency. In an ultra-wideband system, the RF lens antenna demonstrates beam-squint for different reasons from that for the phased array. The lens material is the leading cause of beam-squint, and we apply the Drude–Lorentz model [11] that is suitable for explaining dielectric material. Based on Snell's law, an EM wave is refracted while passing through a dielectric lens owing to the refractive index of the lens expressed as a permittivity. According to the Drude-Lorentz model, the refraction is caused by the fact that permittivity is a function of frequency, which is one of the causative factors that result in beam-squint. However, permittivity is not linear owing to the damping constant and resonance frequency, which are inherent to the material itself. Therefore, accurate values should be obtained by experiments. Permittivity consists of real and imaginary parts. The real part is the dielectric constant, and the tangent loss is the ratio of the real to imaginary parts.

Table I
(ABOVE) ANGLE DISTORTION VALUES [°] IN EVALUATION METHOD 1 (EM1) AND EVALUATION METHOD 2 (EM2)
(BELOW) POWER DIFFERENCE VALUES [DBI] IN EVALUATION METHOD 1 (EM1) AND EVALUATION METHOD 2 (EM2).

Phased array	**27 GHz**		**27.5 GHz**		**28 GHz**		**29 GHz**		**29.5 GHz**		**30 GHz**	
AoD†	*EM1.*	*EM2.*	*EM1.*	*EM2.*	*EM1.*	*EM2.*	*EM1.*	*EM2.*	*EM1.*	*EM2.*	*EM1.*	*EM2.*
6 deg	-0.18		-0.12		-0.06		0.06		0.11		0.16	
12 deg	-0.55		-0.36		-0.18		0.17		0.33		0.48	
18 deg	-0.92	*	-0.60	*	-0.30	*	0.28	*	0.55	*	0.82	*
24 deg	-1.32		-0.87		-0.43		0.40		0.80		1.18	
30 deg	-1.76		-1.15		-0.57		0.54		1.06		1.56	

RF lens	**27 GHz**		**27.5 GHz**		**28 GHz**		**29 GHz**		**29.5 GHz**		**30 GHz**	
AoD†	*EM1.*	*EM2.*	*EM1.*	*EM2.*	*EM1.*	*EM2.*	*EM1.*	*EM2.*	*EM1.*	*EM2.*	*EM1.*	*EM2.*
6 deg	-1.19		-0.03		-0.97		-0.81		-0.13		-0.16	
12 deg	-0.37		-0.11		-0.48		-0.46		0.15		-0.47	
18 deg	0.03	**	-0.01	**	-0.18	**	-0.30	**	-0.16	**	-0.20	**
24 deg	-0.23		0.01		-0.20		-0.11		-0.23		-0.09	
30 deg	0.12		0.61		0.35		0.50		0.20		0.49	

Phased array	**27 GHz**		**27.5 GHz**		**28 GHz**		**29 GHz**		**29.5 GHz**		**30 GHz**	
AoD†	*EM1.*	*EM2.*	*EM1.*	*EM2.*	*EM1.*	*EM2.*	*EM1.*	*EM2.*	*EM1.*	*EM2.*	*EM1.*	*EM2.*
6 deg	0.4		0.2		-0.0		0.0		0.2		0.4	
12 deg	0.5		0.2		-0.1		0.1		0.2		0.4	
18 deg	0.6	0	0.2	0	0.1	0	0.0	0	0.2	0	0.3	0
24 deg	0.7		0.3		0.1		0.0		0.2		0.3	
30 deg	1.0		0.5		0.2		-0.0		-0.0		0.2	

RF lens	**27 GHz**		**27.5 GHz**		**28 GHz**		**29 GHz**		**29.5 GHz**		**30 GHz**	
AoD†	*EM1.*	*EM2.*	*EM1.*	*EM2.*	*EM1.*	*EM2.*	*EM1.*	*EM2.*	*EM1.*	*EM2.*	*EM1.*	*EM2.*
6 deg	0.1		-0.2		0.2		0.4		0.2		0.4	
12 deg	0.0		-0.1		-0.4		-0.3		0.3		-0.2	
18 deg	0.3	‡	0.0	‡	0.0	‡	-0.4	‡	0.1	‡	-0.3	‡
24 deg	0.1		-0.2		-0.3		-0.6		-0.3		-0.7	
30 deg	-0.6		-0.2		-0.9		-0.1		-0.1		0.9	

All values in the tables are the difference values from the standard frequency at 28.5 GHz.
† indicates Tx beamforming direction in the azimuth angle of antenna via analog beamforming.
* indicates that the values are not changed from *Evaluation method 1* to *Evaluation method 2*.
** $< .001$
‡ $< .01$

As noted above, the refractive index of the lens can be expressed in terms of permittivity. It can be observed that the real part of the refractive index accounts for the beam refraction. Because the permittivity influences the real part of the refractive index, the other frequency bands pass through the material but with different degrees of refraction, resulting in beam-squint at the lens. The permittivity affects the refractive index, so it is advantageous to have fewer dielectric-constant-and-tangent-loss variations in the operating frequency band. Therefore, it is essential to select the lens material with fewer permittivity variations in the lens-based BF system.

B. Lens Antenna Structure

In Fig. 1, the RF lens antenna consists of two parts: the antenna array connected with RF chains and the lens structure in the front end of the antenna array. The lens structure is used to focus the beam generated by the antenna array for an analog BF. A beam steering is achieved using the lens refractions with the on-off switching of the antenna [12]. To reduce hardware complexity and allow faster beam tracking than phase-shifted array, there are advantages to switching BF using one element or a subset of the antenna array [7].

According to Section II-A, the refractive index of the lens must be a function of frequency. When engineers select the material to use in manufacturing the lens, they should take into account the beam-squint phenomenon. In designing the RF lens in our previous study, we considered five materials– Teflon type A, polyethylene, polycarbonate, Boron Nitride, and MgO. We need to consider whether these materials have stable dielectric constants and tangent loss values. However, for most of the RF lens materials in the mmWave band, there exists no precisely and densely sampled dielectric constant and tangent loss data through measurements. In this paper, the lens material used in the simulation is Teflon type A. The author of [13] used the open resonator method suitable for measuring complex permittivity in the 15-65 GHz band. The permittivity of Teflon type A is approximately 2.03 in wideband, and the loss tangent values vary from 0.000147 to 0.000216. As such, Teflon type A has small loss tangent values and does not have large deviations in the permittivity from the 27 GHz to the 30 GHz range. These characteristics of Teflon work in favor of the lens to mitigate beam-squint. In this paper, we use a hyperbolic curve shape of the lens based on [12].

III. BEAM-SQUINT ANALYSIS BASED ON 3D EM ANALYSIS SOFTWARE

In this section, to analyze the beam-squint phenomenon in the RF lens and the phased array, we use the 3D EM

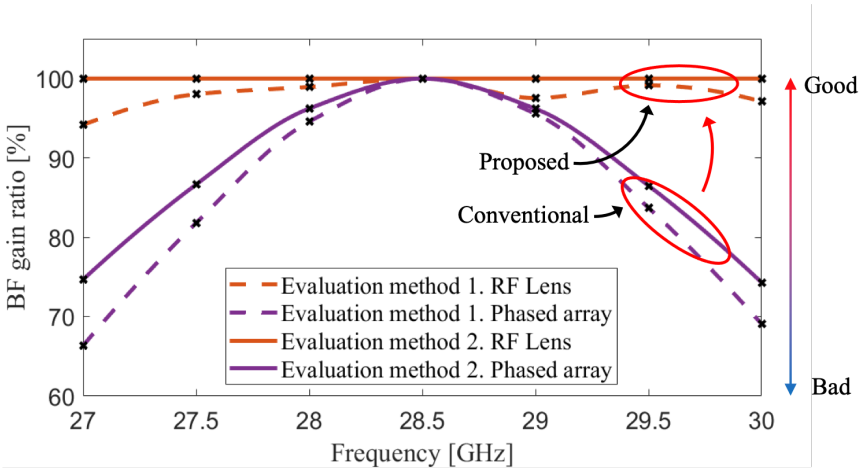

Figure 2. The BF gain ratio along the frequency caused by the beam-squint from the 3D EM simulation.

simulation, CST Studio Suite. We introduce the assessment model in Sections III-A and III-B and present our simulation results in Section III-C.

A. Beam-squint Assessment Model

For an accurate analysis of the beam-squint, we set two evaluation models. Evaluation model 1 takes into account only *Assumption 1*. Evaluation model 2 considers *Assumptions 1* and *2*. The assumptions are as follows:

Assumption 1: In an RF lens, the factor that affects beam refraction is only the refractive index, which is a function of permittivity. *Assumption 2*: The antenna gain of the antenna elements in the uniform linear array (ULA) is consistent for the ultra-wideband. *Assumption 1* is designed to eliminate the likelihood of intervention by other variables in the refractive index. *Assumption 2* removes the distorted components according to the narrowband antenna elements. In Evaluation model 2, we can observe the beam-squint phenomenon due to the inherent causative factors, excluding external causative factors such as the narrowband antenna elements.

B. Parameters and Degraded Power Caused by Beam-squint for Analysis

As the beam-squint occurs, the BF gain is degraded. This degraded gain leads to a degraded received power. From the perspective of the transmitter then, we analyze the extent of the attenuated BF gains. To assess the beam-squint phenomenon, we introduce several parameters. The first is angle distortion (AD). AD is the difference between the azimuth angle at peak BF gain for the operating frequency and the center frequency. The second parameter is power difference (PD); PD represents the difference between the peak BF gain at each operating frequency and the center frequency. The third parameter is the half-power beamwidth (HPBW) of the beam at each frequency band. The HPBW depends on the array size, with a larger array size resulting in a narrower beam, leading to critical mis-alignment. Evaluating beam-squint by merely AD cannot accurately account for the performance attenuation. Hence, we add PD and HPBW to provide the BF gain ratio and received power ratio that evaluate more general and accurate beam-squint performance.

Based on the direction of the analog beam at the center frequency, the BF gain ratio is defined as the percentage of the ratio of the directivity gain at the center frequency to the mis-aligned directivity gain at the operating frequency. For example, an 80% BF gain ratio value at 27 GHz implies that the antenna gain at 27 GHz in the direction aligned with 28.5 GHz is 80% of the antenna gain at 28.5 GHz.

C. AD, PD, and BF gain ratio Assessment Comparison for Phased Array with The RF Lens in a ULA

We simulated two different antenna structures–an RF lens and a phased array in 20λ antenna diameters, where λ is a wavelength at the center frequency. The 20λ arrays consist of 28x1 patch antennas with $\frac{\lambda}{2}$ distance between two adjacent patch antennas. Table I, based on a 3D EM analysis software simulation, shows AD and PD data of the RF lens antennas and the phased array. We analyze Table I data as the phased array, RF lens antenna, and BF gain ratio. Finally, with Table II, we present a summary of the categories of causative factors and affected parameters in each antenna structure. Before analysis, in Table I, the y-axis represents the angle of departure (AoD) of Tx analog BF, and the x-axis represents operating frequencies from 27 GHz to 30 GHz without 28.5 GHz. The data in the tables consist of AD and PD values introduced in Section III-B; all data are calculated difference values from the center frequency, 28.5 GHz.

Phased array: According to Evaluation method 1 data, shown above in Table I, AD in the phased array becomes more distorted as the frequency gets further away from the center frequency. This is because the steering vector set for the center frequency causes angle distortion at different operating frequencies. In addition, AD becomes more distorted as the AoD increases. Hence, maximum distortion values are -1.76° (30°, 27 GHz) and 1.56° (30°, 30 GHz). It is worth noting that data from Evaluation method 2 is the same as that from Evaluation 1. Table I (below) shows PD values. Existing PD values in Evaluation method 1 become zero values in Evaluation method 2. These data imply that PD in a phased

Table II
A CATEGORY OF CAUSATIVE FACTORS FOR BEAM-SQUINT IN EVALUATION METHOD 1 AND 2.

Category of causative factors	**Causative factor**	**Affected parameters**	**Evaluation method**	
Inherent factors of the **phased array** structure	Array size	HPBW	**Evaluation method 1**	**Evaluation method 2**
	Steering vector	Angle distorstion		
Inherent factors of the **RF lens** structure	Array size	HPBW		
	Frequency-dependent permittivity	Angle distortion		
		Power difference		
External common factor	Narrowband antennas in the ULA†	Angle distortion		–
		Power difference		

† The antenna gain of a narrowband antenna element in the ULA is not consistent for the ultra-wideband.

array is affected by a narrowband antenna beam pattern as an external factor only. In the phased array, however, AD does not depend on that external factor.

RF lens antenna: According to the evaluation method 1 data shown above in Table I, we can see that the AD values of the RF lens are not consistent. For those causative factors that caused some distortion, we can see the evaluation method 2 data where AD values of RF lens are less than 0.001 that are both independent on AoD and frequencies. This data analysis implies that most of the causative factors that cause AD are the inconsistent antenna gains across the frequency band. In Table I (below), the PD of the RF lens has the same result. The PD values of Evaluation method 1 in RF lens are less than 0.01. This result implies that the most causative factor causing PD is the narrowband antenna as an external factor, not an RF lens's inherent factor. The remaining values are caused by the frequency-dependent permittivity introduced in Section II-A.

A summary of the causative factors in each antenna: We analyze and summarize causative factors and affected parameters (AD, PD, HPBW) based on Table I data for phased array and RF lens antenna. In Table II, causative factors are classified as either inherent or external. An inherent factor concerns a structural feature of the antenna that gives rise to the beam-squint phenomenon. Evaluation method 1 contains two types of causative factors, and Evaluation method 2 analyzes only the inherent factors. An inherent factor of the phased array structure is the steering vector that affects AD. In the RF lens structure, a causative factor is the frequency-dependent permittivity, and it affects AD and PD. In the external factor category, a narrowband antenna affects the PD of the phased array and the AD and PD of the RF lens. Especially in the RF lens, the external factor constitutes the most causative factor. Hence, the RF lens array that uses ideal or ultra-wideband antenna elements has robustness for the beam-squint.

BF gain ratio: We analyze degraded BF gain by converting Table I data to BF gain ratio. Fig. 2 presents the BF gain ratio along with the frequency. The solid lines signify Evaluation method 1 and the dashed lines signify Evaluation method 2. The BF gain ratio from the proposed RF lens is much less degraded than that of the conventional phased array. In Evaluation method 1, we can see that the phased array has only 67% and 69% BF gain of standard BF gain (at the center frequency) at 27 GHz and 30 GHz. In Evaluation method 1, by contrast, the RF lens's BF gain ratios have over 93% of the minimum value. In Evaluation method 2, the RF lens is almost free of BF gain attenuation by the beam-squint by excluding an external factor.

IV. SYSTEM-LEVEL AND LINK-LEVEL ASSESSMENTS

This section presents the evaluations of the spectral efficiency and received power ratio at the system and link-levels. Note that the system-level simulation is based on the antenna patterns of CST simulation in Section III. Furthermore, we use the received power ratio instead of the BF gain ratio. The received power ratio is defined as the ratio of received powers based on distorted AD, PD, and HPBW, similar to the BF gain ratio.

A. System-Level Performance Analysis and Evaluation

We evaluate the RF lens-embedded system and phased array with a system-level simulator using Wireless System Engineering (WiSE)–a 3D ray tracing tool developed by Bell Labs [14]. For realistic performance evaluations, we model a building in a university, as shown in Fig. 3 (above right). The simulation area is indoors with a line-of-sight (LoS) environment to consider the beam-squint phenomenon and straightness characteristics of the mmWave signal. With the multiuser environment, we assume perfect channel state information (CSI) in all Rx locations. With this assumption, we adopt the best beam selection (BBS) method to choose the best beam for each user according to received power. As shown in Table I, because the AD unit is 0.01°, we set a 0.01 m distance for accurate received power and high resolution of AoD estimations. In Fig. 3 (above right), the BS (marked by a blue star) steers the ten beams between 0° and 30° towards the left in the simulated space. To estimate the received power ratio, and spectral efficiency, the received power for the other frequencies of a selected beam at each location is aggregated. In the two Evaluation methods, we analyze the two types of antennas. The detailed system parameters are given in Fig. 3 (left).

In the simulation, each user selects the best beam based on the center frequency at each UE position. However, though the beam was selected based on the center frequency, the overall received power is attenuated by ADs and PDs at

PARAMETERS IN THE SYSTEM-LEVEL SIMULATION

Parameters		Value
mmWave carrier frequency		28.5 GHz
System bandwidth		3 GHz (27∼30 GHz)
# of Sampled frequency band		7
Sample frequency spacing		500 MHz
Antenna type	BS	RF lens array (20λ) Phased array (20λ)
	UE	Isotropic antenna
The number of beams		10
Scanning angle (Azimuth)		0∼30°
BS and UE height		1 m
Transmit power		23 dBm
UE grid spacing		0.01 m
Thermal noise		-79 dBm
Indoor map size	Width	10 m
	Depth	20 m
	Height	3 m

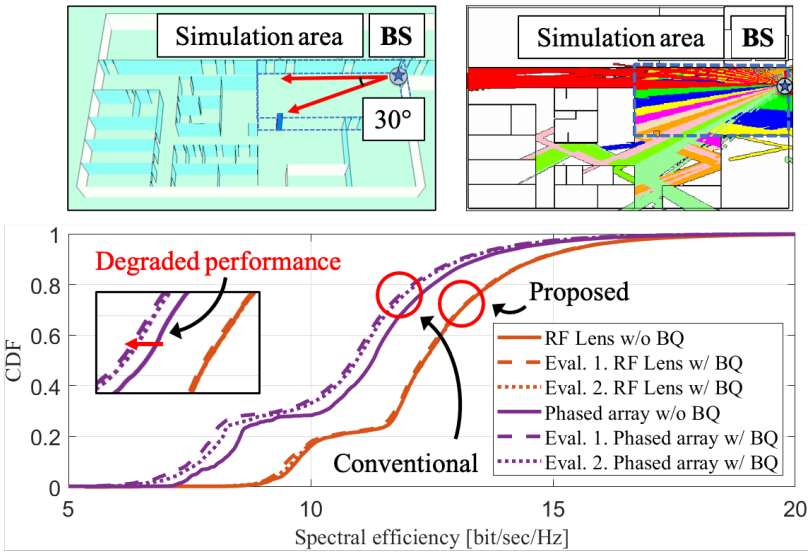

Figure 3. (left) Parameters in the system-level simulation; (right-above) The indoor map of 3D ray tracing system-level simulation. Each color means the best beams which are selected using the Best Beam Selection method among the ten beams (0 ∼ 30°); (right-below) Degraded spectral efficiency assessment due to beam-squint for the conventional and proposed antennas.

the other operating frequencies, depending on the beam-squint phenomenon. Fig. 3 (below right) presents the spectral efficiencies for the system-level simulation. In the spectral efficiency graphs, the solid line indicates the spectral efficiency without the beam-squint phenomenon. The dashed and dotted lines indicate Evaluation model 1 and Evaluation model 2, respectively. In Fig. 3 (below right), the phased array in Evaluation model 1 (represented as the dashed line) demonstrates a 1.11 dB degradation relative to the scenario without beam-squint (represented as the solid line). Furthermore, the phased array in Evaluation model 2 shows a degradation of 0.87 dB. In the case of the RF lens, the deterioration in system performance is minimal. Evaluation model 1 shows a degradation of 0.12 dB, but Evaluation model 2 has no deterioration compared with the solid line. It is worth noting that the spectral efficiency of the lens antenna system is higher at 2 bit/s/Hz than that of the phased array. Although the same power is used in both systems, the lens antenna with the beam-focusing characteristic performs twice as good as the phased array.

In conclusion, it is impossible in the hybrid BF system to entirely compensate for the AD and PD of the phased array without increasing hardware complexity. The phased array structure, therefore, has an inherent limitation for the beam-squint phenomenon. In contrast, the beam-squint problem of the RF lens system can, with stable permittivity materials, be negligible.

B. Link-Level Performance Analysis and Evaluation

1) System Configuration: To test the lens antenna performance as a component of a transmission system, we evaluated its link-level performance using the mmWave transceiver system software-defined radio (SDR) platform [15]. The communication system consists of a LabVIEW system design software and PXIe SDR. As shown in Fig. 4 (above left), the Tx node (as a BS) and Rx node (as a UE) are separated by 5m. The Tx consists of an IF-LO module, I/Q-generator, and Tx NI up-converter. The Rx consists of an IF-LO module, I/Q-digitizer, decoder, multiple-access channel, and Rx down-converter. The fabricated lens antenna is used in the BS with uplink and downlink frequencies of 28.5 GHz and 800 MHz bandwidth each. We test the link-level performance when the lens antenna is a transmitter, and the feed horn antenna is a receiver. A single data stream is transmitted and received via a modulation and coding scheme, more specifically, a 64-quadrature amplitude modulation. The detailed parameters are given in Fig. 4 (above right). Fig. 4 (below left) shows the fabricated RF lens antenna used in the BS. The fabricated lens material is polycarbonate, not Teflon type A. The diameter of the RF lens is 4.5λ. Because we use a different RF lens, the results in Fig. 4 (below right) are different from the system-level simulation results in Section IV-A. However, this demonstration is performed in the same environment as that used for the system-level simulation. We verify the beam-squint phenomenon of the fabricated lens in terms of its AD, PD, and received power ratio. In this demonstration, the analog BF's AoD is 9.26°. We measure the received powers at 27.5 GHz, 28.5 GHz, and 29.5 GHz.

2) MmWave Link-Level Beam-squint Performance Assessment: Here, the received power ratio values are empirically demonstrated for assessing performance degradation due to beam-squint in the indoor link-level testbed. The testbed verifies the existence of beam-squint in the fabricated lens antenna. As a result, Fig. 4 (below right) illustrates the AD, PD, and received power ratio from a beam-squint perspective. The AoD changes are 0.26° at 27.5 GHz and 0.08° at 29.5 GHz. The HPBW of the fabricated lens is 15°. Regarding the received power ratio, this RF lens shows a percentage of 91.98% and 91.99% at 27.5 GHz and 29.5 GHz, respectively.

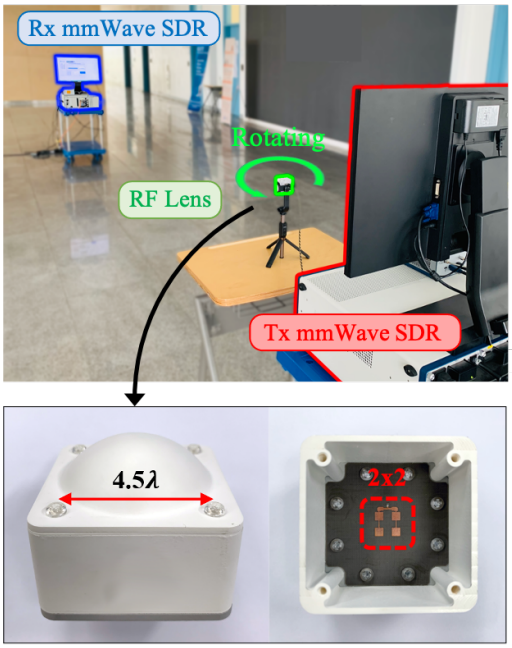

PARAMETERS IN THE LINK-LEVEL DEMONSTRATION

Parameters	Value	Parameters		Value
Carrier frequency	28.5 GHz	Antenna type	BS	1 x RF lens
System bandwidth	800 MHz		UE	1 x Horn
# of sampled frequency	3	RF lens antenna	HPBW	15° ± 4
Sample frequency spacing	1 GHz		Gain	18 dBi
Waveform	CP-OFDM		Diameter	4.5λ
FFT Size	2048 @ 75 kHz subcarrier spacing		Material	Polycarbonate
		Tx RX height		1 m
Duplexing	Dynamic TDD	Tx Rx distance		5 m
Modulation	64-QAM	Analog direction		9.26°
MIMO Scheme	Hybrid beamforming	# of bounces		2
Coding	Turbo	Transmit power		23 dBm

BEAM-SQUINT RESULTS OF THE FABRICATED RF LENS VIA MMWAVE HARDWARE TESTBED

Freqency	AoD[1,*]	Received power[2,**]	AD*	PD**	Received power ratio†
27.5 GHz	9.52	-6.9	-0.26	-0.6	91.98
28.5 GHz	9.26	-7.5	0	0	100
29.5 GHz	9.34	-6.9	-0.08	-0.6	91.99

[1] indicates the direction of analog beamforming in azimuth.
[2] indicates the maximum received power of [1].
*, **, † Units are [°], [dBm], and [%], respectively.

Figure 4. (left-above) Indoor mmWave software-defined radio (SDR) testbed with a fabricated RF lens for beam-squint; (left-below) Fabricated RF lens antenna with polycarbonate; 2x2 patch antenna inside lens structure; (right-above) Parameters in the link-level demonstration; (right-below) Beam-squint results of the fabricated RF lens via mmWave hardware testbed

V. CONCLUSION

This study investigated the beam-squint phenomenon of a phased array and an RF lens antenna in an ultra-wideband mmWave system. Our work analyzed, in a convex RF lens-based hybrid BF system, the causative factors for the beam-squint problem, separated by inherent causative factors and an external factor. Using 3D electromagnetic analysis software, we compared and analyzed the phased array and the lens antenna under the same conditions in terms of beam-squint with the BF gain and the received power. Through the analysis, we manifested that the beam-squint problem of the RF lens system can be negligible with stable permittivity materials. Then, using 3D ray tracing in an indoor environment, we showed the degraded spectral efficiency, caused by beam-squint, for both the phased array and the RF lens antenna. Finally, we demonstrated the indoor mmWave link-level with the fabricated RF lens and verified the performance degradation owing to the beam-squint.

REFERENCES

[1] F. Boccardi *et al.*, "Five disruptive technology directions for 5G,'' *IEEE Commun. Mag.*, vol. 52, no. 2, pp. 74–80, Feb. 2014.

[2] "3GPP TR 21.915 v15.0.0.," *Technical Specification Group Services and System Aspects; Release 15 Description*, p. 35, Sept. 2019.

[3] D. Gesbert *et al.*, "Shifting the MIMO paradigm," *IEEE Signal Process. Mag.*, vol. 24, no. 5, pp. 36–46, Oct. 2007.

[4] R. W. Heath, Jr. *et al.*, "An overview of signal processing techniques for millimeter wave MIMO systems," *IEEE J. Sel. Topics Signal Process.*, vol. 10, no. 3, pp. 436–453, Apr. 2016.

[5] O. El Ayach *et al.*, "Low complexity precoding for large millimeter wave MIMO systems," in *Proc. IEEE Int. Conf. on Commun. (ICC)*, pp. 3724–3729, Jun. 2012.

[6] J. Brady, N. Behdad, and A. M. Sayeed, "Beamspace MIMO for millimeter-wave communications: System architecture, modeling, analysis, and measurements," *IEEE Trans. Antennas Propag.*, vol. 61, no. 7, pp. 3814–3827, Jul. 2013.

[7] Y. Zeng and R. Zhang, "Millimeter wave MIMO with lens antenna array: A new path division multiplexing paradigm," *IEEE Trans. Commun.*, vol. 64, no. 4, pp. 1557–1571, Feb. 2016.

[8] B. Wang *et al.*, "Spatial-and frequency-wideband effects in millimeter-wave massive MIMO systems," *IEEE Trans. Signal Process.*, vol. 66, no. 13, pp. 3393–3406, May 2018.

[9] Z. Wang *et al.*, "Digital compensation wideband analog beamforming for millimeter-wave communication," in *Proc. IEEE Veh. Technol. Conf. (VTC Spring)*, pp. 1–5, Jun. 2018.

[10] X. Gao *et al.*, "Wideband beamspace channel estimation for millimeter-wave MIMO systems relying on lens antenna arrays," *IEEE Trans. Signal Process.*, vol. 67, no. 18, pp. 4809–4824, Jul. 2019.

[11] H. A. Lorentz, *The Theory of Electrons: and Its Applications to the Phenomena of Light and Radiant Heat*, Sydney: Wentworth Press, 2019.

[12] T. Kwon *et al.*, "RF lens-embedded massive MIMO systems: Fabrication issues and codebook design," *IEEE Trans. Microw. Theory Tech.*, vol. 64, no. 7, pp. 2256–2271, Jun. 2016.

[13] G. Oliver, "Low-loss materials in high frequency electronics and the challenges of measurement," report, DuPont, Feb. 2015.

[14] Y.-G. Lim *et al.*, "Map-based millimeter-wave channel models: An overview, hybrid modeling, data, and learning," *IEEE Wireless Commun.*, vol. 27, no. 4, pp. 54–62, Aug. 2020.

[15] M. Chung *et al.*, "Prototyping real-time full duplex radios," *IEEE Commun. Mag.*, vol. 53, no. 9, pp. 56–63, Sept. 2015.